

# Effect of Different Alkyl Groups at the N-Position on the Luminescence of Carbazole-Based $\beta$ -Diketonate Europium(III) Complexes

Pei He,<sup>†</sup> Huihui Wang,<sup>†</sup> Shenggui Liu,<sup>†,‡</sup> Jianxin Shi,<sup>†</sup> Gang Wang,<sup>†</sup> and Menglian Gong<sup>\*,†</sup>

State Key Laboratory of Optoelectronic Materials and Technologies, Ministry of Education Laboratory of Bioinorganic and Synthetic Chemistry, School of Chemistry and Chemical Engineering, Sun Yat-sen University, Guangzhou 510275, P. R. China, and School of Chemistry Science and Technology, Zhanjiang Normal University, Development Center for New Materials Engineering and Technology in Universities of Guangdong, Zhanjiang 524048, PR China

Received: July 9, 2009; Revised Manuscript Received: September 21, 2009

A series of carbazole-based  $\beta$ -diketone derivatives and their europium(III) ternary complexes  $\text{Eu}(\text{N-Cx})_3\text{phen}$  were designed and synthesized, where N-Cx denotes carbazole-based  $\beta$ -diketonates with different alkyl substituents at N-position of the carbazole ring and phen is 1,10-phenanthroline. Thermogravimetric analysis (TGA) shows that the decomposition temperature of the complexes is over 360 °C. UV–visible absorption spectroscopy, photoluminescence (PL), and the luminescence quantum yield of the Eu(III) complexes were measured and compared with each other, and the effect of different substituted-alkyls at N-position in the carbazole ring on the photoluminescence was discussed in details, indicating there exists a competition between the absorption capacity and the energy transfer efficiency for the complexes when the structure of the substituted-alkyls changes. The triplet state energy levels of the  $\beta$ -diketonate ligands in the complexes are higher than that of the lowest excited level of  $\text{Eu}^{3+}$  ion,  $^5\text{D}_0$ , so the photoluminescence mechanism of the Eu(III) complexes was proposed as a ligand-sensitized luminescence process. Red LEDs were fabricated by precoating the complexes onto 395 nm emitting InGaN chips. All the results show that this series of Eu(III) complexes is a promising candidate as a red component in fabrication of NUV-based white LEDs.

## Introduction

Carbazole-based compounds are excellent optical and electronic materials such as photoconductivity and photorefractivity,<sup>1</sup> their metal complexes show interesting and unique chemical and physical properties and possess good thermal stability.<sup>2–8</sup> Much attention has been paid on carbazole-based compounds because of the following reasons: (1) 9H-carbazole is a very cheap starting material; (2) it is a fully aromatic unit providing a better chemical and environmental stability; (3) the nitrogen atom can be easily substituted with a wide variety of functional groups to tune the optical and electrical properties.<sup>9</sup>

In recent years, europium(III) organic  $\beta$ -diketonate complexes as red phosphor in the fabrication of white light emitting diodes (LEDs) became attractive because of their wide excitation band, high quantum yields and good color purity.<sup>10–15</sup> Among those Eu(III)  $\beta$ -diketonate complexes, carbazole-based complexes are outstanding for various modifications. There are also some reports on influence of different substituents at 3, 6 or 2, 7 positions.<sup>16</sup> Despite the H atom at the N position of a carbazole ring being the most active, to our best knowledge, there is no report on the effect of different alkyls substituted at nitrogen atom position on the photoluminescence properties of the corresponding Eu(III) complexes.

In this article, a series of carbazole-containing  $\beta$ -diketonates with different alkyl substituents at N-position of the carbazole ring, methyl, ethyl, propyl, and amyl, and the corresponding Eu(III) ternary complexes were designed and synthesized, and the effect of the structure of the various substituents on the

photoluminescence properties of the complexes were investigated. Finally, red LEDs were fabricated by precoating the Eu(III) complexes onto 395 nm emitting InGaN chips.

Figure 1 shows the structure of the synthesized carbazole-containing  $\beta$ -diketonates and 1,10-phenanthroline (phen) used as ligands in this study, where the  $\beta$ -diketonates are 4,4,4-trifluoro-1-(9-methyl-9H-carbazol-3-yl)butane-1,3-dione (N-C1), 4,4,4-trifluoro-1-(9-ethyl-9H-carbazol-3-yl)butane-1,3-dione (N-C2), 4,4,4-trifluoro-1-(9-propyl-9H-carbazol-3-yl)butane-1,3-dione (N-C3), and 4,4,4-trifluoro-1-(9-pentyl-9H-carbazol-3-yl)butane-1,3-dione (N-C5).

## Experimental Section

All reagents and materials are of analytical grade. Solvents were freshly distilled and dried by standard methods.

LED fabrication: the synthesized Eu(III) complex powders were mixed with a silica gel, then were coated onto the surface of the LED chip.

Elemental analysis for the synthesized organic compounds and the complexes was carried out with an Elementar vario EL elemental analyzer. EI-MS spectra were performed on a Thermo DSQ EI-mass spectrometer. <sup>1</sup>H NMR spectra were recorded on a Varian INOVA500NB. Thermogravimetric analysis (TGA) was carried out up to 930 °C with a heating speed of 10.0 K/min in air atmosphere on a Netzsch TG-209 thermogravimetric analyzer. Photoluminescence excitation (PLE) and emission (PL) spectra were measured on an EDINBURGH FLS 920 combined fluorescence lifetime and steady state spectrophotometer equipped with thermo-electric cooled red sensitive PMT (Edinburgh Instruments). The silts of this equipment are controlled for a suitable output display range of intensity and are fixed for the

\* Corresponding author. E-mail: cesgml@mail.sysu.edu.cn.

<sup>†</sup> Sun Yat-sen University.

<sup>‡</sup> Zhanjiang Normal University.

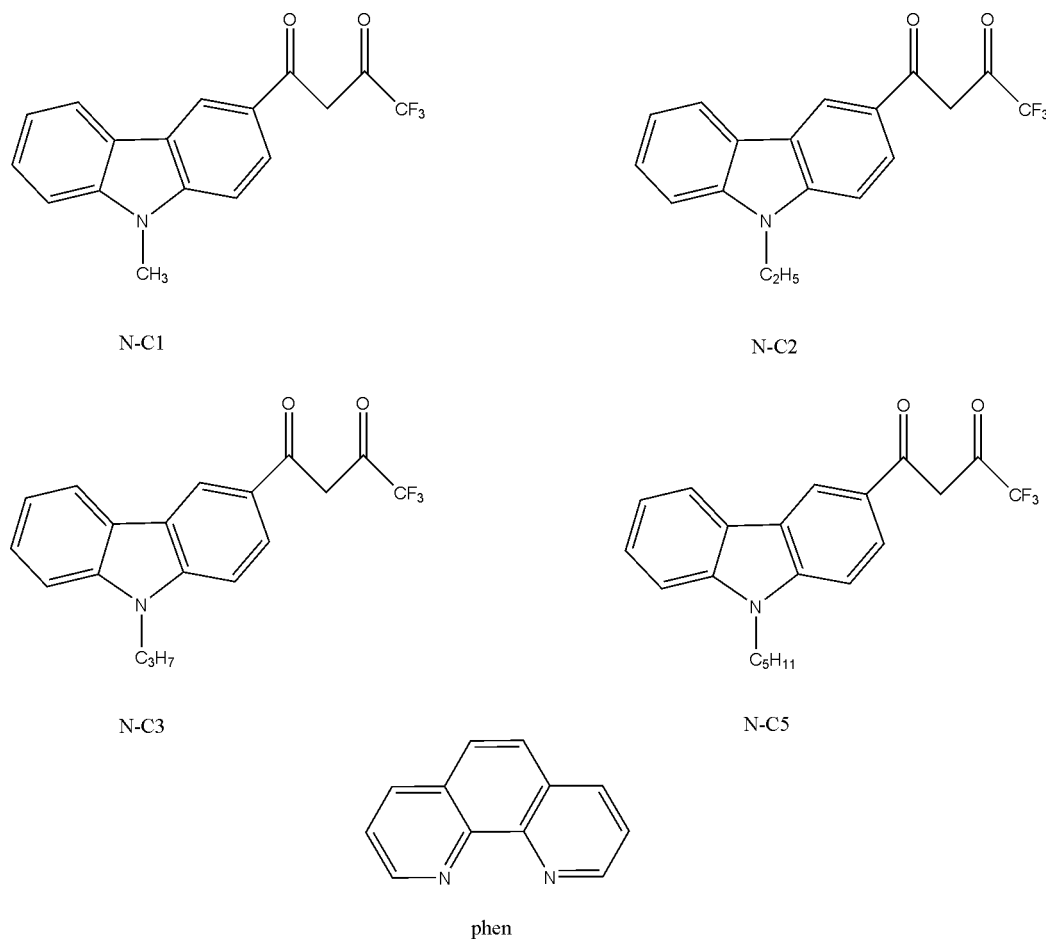


**Figure 1.** Structure of different carbazole-based  $\beta$ -diketones and 1,10-phenanthroline.

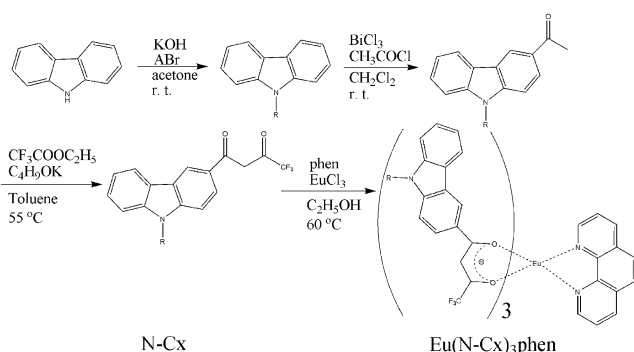


**Figure 2.** Synthesis routine of *N*-substituted carbazole-based  $\beta$ -diketone derivatives and the corresponding Eu(III) ternary complexes.

series of samples in the whole measurement process. UV–visible absorption spectra were recorded on a UV-2501PC UV–visible spectrophotometer. The emission spectra of the fabricated LEDs and the quantum yield of the complexes were measured with an EVERFINE PMS-80 PLUS UV–vis–near IR Spectrophotometer.

The synthesis routine for the carbazole-based  $\beta$ -diketone ligands and the Eu(III) ternary complexes is shown in Figure 2.

Methylcarbazole was purchased from Merger Co.; other *N*-substituted carbazoles were synthesized from carbazole. The synthesis routine of the compounds and their Eu(III) complexes is analogous to the method described in our earlier work,<sup>13</sup> and the products were confirmed by EI-MS spectra, <sup>1</sup>H NMR spectra, and elemental analysis.

KOH (50 mmol) and acetone (80 mL) were mixed together, and the mixture was stirred for 20 min; then carbazole (40 mmol)

was added into and stirring was continued for 40 min. A mixture of brominated alkane (alkane is ethyl, propyl, or amyl, respectively) (60 mmol) in acetone was added dropwise into the solution. The reaction solution was refluxed 3 days, then poured into a mixture of ice and water, and stirred continuously until a white precipitate was deposited completely. The precipitate was then filtered, washed with deionized water, and recrystallized from alcohol (90% yield for ethylcarbazole, 84% for propylcarbazole, and 78% for amylcarbazole).

All the ketones were synthesized by using BiCl<sub>3</sub> as catalyst in the acylation reaction. *N*-Alkyl substituted carbazole (10 mmol) and BiCl<sub>3</sub> (16 mmol) were added in anhydrous CH<sub>2</sub>Cl<sub>2</sub> (25 mL). Then a mixture of acetyl chloride (1.75 mL) in anhydrous CH<sub>2</sub>Cl<sub>2</sub> (7.5 mL) was added dropwise into the solution and stirred for 12 h. Diluted hydrochloric acid (7.5 mol/L, 20 mL) was added and stirred until a precipitate was dissolved fully. The mixture was extracted with CH<sub>2</sub>Cl<sub>2</sub>. The organic extract was evaporated in vacuum and the crude product was purified by column chromatography (petroleum ether–CH<sub>2</sub>Cl<sub>2</sub>) to give the pure ketones (65% for 3-acetyl-9-methyl carbazole, 75% for 3-acetyl-9-ethyl carbazole, 68% for 3-acetyl-9-propyl carbazole, and 69% for 3-acetyl-9-amyl carbazole).

A mixture of the ketone (5 mmol), toluene (20 mL), CF<sub>3</sub>COOC<sub>2</sub>H<sub>5</sub> (1.2 mL), and C<sub>4</sub>H<sub>9</sub>OK (0.8 g) were stirred and heated at 50 °C and reflux for 12 h under a N<sub>2</sub> atmosphere. After cooling, the mixture was treated with hydrochloric acid (1 mol/L 30 mL) and extracted with toluene. The solvent was evaporated in a vacuum. The crude product was purified by column chromatography over silica gel and then recrystallized from alcohol to give the pure products of the substituted

carbazole  $\beta$ -diketones (N-Cx) (88% for N-C1, 97% for N-C2, 78% for N-C3, and 77% for N-C5).

N-Cx and phen were solved in alcohol, a solution of  $\text{EuCl}_3$  in alcohol was added, the mixture was stirred and heated at 60 °C until all reagents were solved. The pH value of the solution was controlled between 7.0 and 8.0 by adding NaOH or HCl solution. Then the reaction was kept on for 6 h. A yellow precipitate formed and was filtrated, washed with ethanol and deionized water, and dried at 50 °C in vacuum.  $\text{Eu}(\text{N-Cx})_3\text{phen}$  was obtained (83% for  $\text{Eu}(\text{N-C1})_3\text{phen}$ , 87% for  $\text{Eu}(\text{N-C2})_3\text{phen}$ , 81% for  $\text{Eu}(\text{N-C3})_3\text{phen}$ , and 81% for  $\text{Eu}(\text{N-C5})_3\text{phen}$ ).

For measuring the lowest triplet state energy levels of the primary ligands N-Cx, gadolinium(III) binary complex with N-Cx,  $\text{Gd}(\text{N-Cx})_3 \cdot 2\text{H}_2\text{O}$ , were also synthesized with a similar procedure except using phen. All the Gd(III) complexes were conformed by the elemental analysis data.

**N-C1.**  $^1\text{H NMR}$  ( $\text{CDCl}_3$ ):  $\delta$  3.893 (s, 3H);  $\delta$  6.698 (s, 1H);  $\delta$  7.323–7.363 (m, 1H);  $\delta$  7.420–7.459 (t, 2H);  $\delta$  7.536–7.578 (m, 1H);  $\delta$  8.67–8.093 (q, 1H);  $\delta$  8.149–8.173 (m, 1H);  $\delta$  8.720–8.725 (t, 1H). MS (EI):  $m/z$  319 ( $\text{M}^+$ ), 250 ( $\text{M}^+ - \text{CF}_3$ ). Elemental analysis data for N-C1 ( $\text{C}_{17}\text{H}_{12}\text{F}_3\text{NO}_2$ ), found (calcd): N, 4.31 (4.39); C, 64.17 (63.95); H, 3.86 (3.79).

**$\text{Eu}(\text{N-C1})_3\text{phen}$ .** Elemental analysis data for  $\text{Eu}(\text{N-C1})_3\text{phen}$  ( $\text{C}_{63}\text{H}_{41}\text{EuF}_9\text{N}_5\text{O}_6$ ), found (calcd): C, 58.65 (58.79); N, 5.41 (5.44); H, 3.38 (3.21).  $^1\text{H NMR}$  (DMSO):  $\delta$  3.89 (s, 9H,  $-\text{CH}_3$ );  $\delta$  4.58 (s, 2H enol- $\gamma$ -CH-);  $\delta$  6.89–7.00 (m, 3ArH);  $\delta$  7.40–7.44 (m, 6ArH);  $\delta$  7.54–7.56 (m, 3ArH);  $\delta$  7.72–8.00 (q; 10ArH);  $\delta$  8.35–8.50 (m; 5ArH);  $\delta$  9.11 (s; ArH). MALDI-MS:  $m/z$  1288 [ $\text{M} + \text{H}$ ] $^+$ , 1310 [ $\text{M} + \text{Na}$ ] $^+$ .

**N-C2.**  $^1\text{H NMR}$  ( $\text{CDCl}_3$ ):  $\delta$  1.45–1.49 (t, 3H);  $\delta$  4.37–4.42 (q, 2H);  $\delta$  6.696 (s, 1H);  $\delta$  7.25–7.57 (q, 4H);  $\delta$  8.05–8.18 (m, 2H);  $\delta$  8.72–8.73 (d, 1H). MS (EI):  $m/z$  333 ( $\text{M}^+$ ), 334 ( $\text{M}^+ + 1$ ), 318 ( $\text{M}^+ - \text{methyl}$ ). Elemental analysis data for N-C2 ( $\text{C}_{18}\text{H}_{14}\text{F}_3\text{NO}_2$ ), found (calcd): N, 4.11 (4.20); C, 64.67 (64.86); H, 4.21 (4.23).

**$\text{Eu}(\text{N-C2})_3\text{phen}$ .** Elemental analysis data for  $\text{Eu}(\text{N-C2})_3\text{phen}$  ( $\text{C}_{66}\text{H}_{47}\text{EuF}_9\text{N}_5\text{O}_6$ ), found (calcd): C, 59.33 (59.58); N, 5.37 (5.27); H, 3.45 (3.57).  $^1\text{H NMR}$  ( $\text{CDCl}_3$ ):  $\delta$  1.41–1.46 (t, 9H  $-\text{CH}_3$ );  $\delta$  3.44 (s, 3H enol- $\gamma$ -CH-);  $\delta$  4.37–4.44 (q, 6H  $-\text{CH}_2$ -);  $\delta$  7.14–7.19 (m, 5ArH);  $\delta$  7.35–7.57 (m, 10ArH);  $\delta$  8.23–8.26 (d, 3ArH);  $\delta$  8.45–8.48 (d, 2ArH);  $\delta$  8.66 (s, 3ArH);  $\delta$  8.83 (d, 2ArH);  $\delta$  9.92 (s, 2ArH);  $\delta$  10.41–10.44 (d, 2ArH). MALDI-MS:  $m/z$  1329 [ $\text{M}$ ] $^+$ , 1352 [ $\text{M} + \text{Na}$ ] $^+$ .

**N-C3.**  $^1\text{H NMR}$  ( $\text{CDCl}_3$ ):  $\delta$  1.98–1.03 (t, 3H);  $\delta$  1.92–1.99 (q, 2H);  $\delta$  4.27–4.32 (t, 2H);  $\delta$  6.69 (s, 1H);  $\delta$  7.26–8.70 (m, 7H). MS (EI):  $m/z$  347 ( $\text{M}^+$ ), 348 ( $\text{M}^+ + 1$ ), 318 ( $\text{M}^+ - \text{ethyl}$ ). Elemental analysis data for N-C3 ( $\text{C}_{19}\text{H}_{16}\text{F}_3\text{NO}_2$ ), found (calcd): N, 3.95 (4.03); C, 65.96 (65.70); H, 4.76 (4.64).

**$\text{Eu}(\text{N-C3})_3\text{phen}$ .** Elemental analysis data for  $\text{Eu}(\text{N-C3})_3\text{phen}$  ( $\text{C}_{69}\text{H}_{53}\text{EuF}_9\text{N}_5\text{O}_6$ ), found (calcd): C, 60.22 (60.44); N, 5.17 (5.11); H, 3.81 (3.90).  $^1\text{H NMR}$  ( $\text{CDCl}_3$ ):  $\delta$  0.92–0.96 (t, 9H  $-\text{CH}_3$ );  $\delta$  1.86–1.91 (q, 6H  $-\text{CH}_2$ -);  $\delta$  3.69 (s, 3H enol- $\gamma$ -CH-);  $\delta$  4.28–4.33 (t, 6H  $-\text{CH}_2$ -);  $\delta$  7.16–7.18 (m, 6ArH);  $\delta$  7.42–7.51 (m, 9ArH);  $\delta$  8.28–8.42 (q, 5ArH);  $\delta$  8.74–8.83 (m, 5ArH);  $\delta$  9.87 (s, 2ArH);  $\delta$  10.35–10.37 (d, 2ArH). MALDI-MS:  $m/z$  1371 [ $\text{M}$ ] $^+$ , 1394 [ $\text{M} + \text{Na}$ ] $^+$ .

**N-C5.**  $^1\text{H NMR}$  ( $\text{CDCl}_3$ ):  $\delta$  0.867–0.902 (m, 3H);  $\delta$  1.347–1.392 (m, 4H);  $\delta$  1.859–1.933 (m, 2H);  $\delta$  4.305–4.342 (t, 2H);  $\delta$  6.699 (s, 1H);  $\delta$  7.314–7.559 (m, 4H);  $\delta$  8.054–8.175 (m, 2H);  $\delta$  8.730–8.734 (d, 1H). MS (EI):  $m/z$  375 ( $\text{M}^+$ ), 376 ( $\text{M}^+ + 1$ ), 318 ( $\text{M}^+ - \text{butyl}$ ). The elemental analysis data for N-C5 ( $\text{C}_{21}\text{H}_{20}\text{F}_3\text{NO}_2$ ), found (calcd): N, 3.721 (3.73); C, 67.21 (67.19); H, 5.534 (5.73).

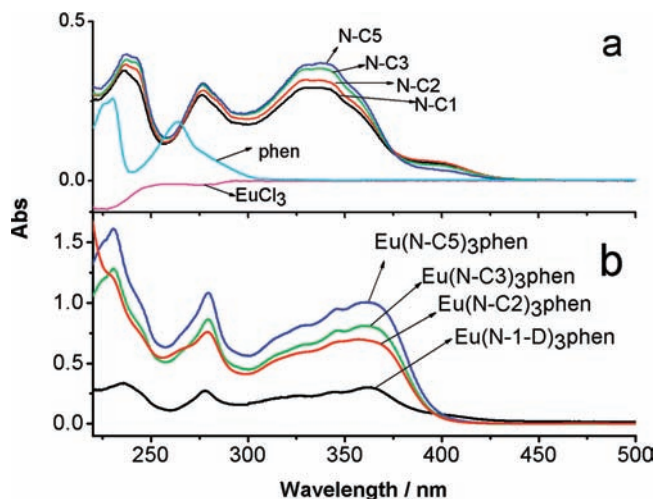


**Figure 3.** UV-vis absorption spectra of the free ligands N-Cx and phen,  $\text{EuCl}_3$  (a) and  $\text{Eu}(\text{N-Cx})_3\text{phen}$  (b) in ethanol ( $1 \times 10^{-5}$  mol/L).

**$\text{Eu}(\text{N-C5})_3\text{phen}$ .** Elemental analysis data for  $\text{Eu}(\text{N-C5})_3\text{phen}$  ( $\text{C}_{75}\text{H}_{65}\text{EuF}_9\text{N}_5\text{O}_6$ ), found (calcd): C, 61.60 (61.90); N, 4.56 (4.81); H, 4.32 (4.50).  $^1\text{H NMR}$  ( $\text{CDCl}_3$ ):  $\delta$  0.85–0.90 (t, 9H  $-\text{CH}_3$ );  $\delta$  1.34 (s, 12H  $-\text{CH}_2$ -);  $\delta$  1.83–1.86 (t, 6H  $-\text{CH}_2$ -);  $\delta$  3.68 (s, 3H, enol- $\gamma$ -CH-);  $\delta$  4.31–4.33 (t, 6H,  $-\text{CH}_2$ -);  $\delta$  7.13–7.19 (m, 6ArH);  $\delta$  7.40–7.43 (m, 6ArH);  $\delta$  7.50–7.53 (m, 3ArH);  $\delta$  8.28–8.30 (d, 3ArH);  $\delta$  8.41–8.43 (d, 2ArH);  $\delta$  8.75–8.83 (m, 5ArH);  $\delta$  9.86 (s, 2ArH);  $\delta$  10.36–10.37 (d, 2ArH). MALDI-MS:  $m/z$  1455 [ $\text{M}$ ] $^+$ , 1488 [ $\text{M} + \text{Na}$ ] $^+$ .

## Results and Discussion

Thermogravimetric analysis (TG-DTG) curves show that the decomposition temperatures of  $\text{Eu}(\text{N-Cx})_3\text{phen}$  ( $x = 1, 2, 3, 5$ ) are 363, 366, 360, and 362 °C, respectively. This means that the different alkyl substituents did not change decomposition temperature obviously, and the all of the complexes are thermally stable enough to be applied in LEDs since LEDs work usually at a temperature below 100 °C.

The UV-visible absorption spectra for the free ligands,  $\text{EuCl}_3$  and  $\text{Eu}(\text{N-Cx})_3\text{phen}$  in ethanol ( $1 \times 10^{-5}$  mol/L) were measured and shown in Figure 3.  $\text{EuCl}_3$  shows little absorption in the UV-visible range while the free ligands N-Cx and phen exhibit strong absorption (see Figure 3a), suggesting that the absorption of the corresponding Eu(III) complexes is attributed to the organic ligands. Formation of the  $\text{Eu}^{3+}$  complexes remarkably enhances the absorption intensity (Figure 3b) compared with the ligands N-Cx and phen while the absorption band of the complexes keeps in a wide range from 200 to 400 nm, which is mostly attributed to the absorption of the principal ligand N-Cx, and the absorption band from the secondary ligand phen is mainly located below 300 nm. However, existence of the secondary ligand phen not only increases the absorption intensity in the range 200–300 nm but also satisfies the high coordination number of 8 of the central  $\text{Eu}^{3+}$  ion, and thus improves the coordination stability and thermal stability of the complexes.

There are few changes in band positions when the alkyl substituent in the carbazole ring is enlarged from methyl to amyl. However, the absorption of  $\text{Eu}(\text{N-Cx})_3\text{phen}$  decreases in the order  $\text{Eu}(\text{N-C5})_3\text{phen} > \text{Eu}(\text{N-C3})_3\text{phen} > \text{Eu}(\text{N-C2})_3\text{phen} > \text{Eu}(\text{N-C1})_3\text{phen}$  since the electron-donating capacity decreases from amyl to methyl; consequently, the electron density is minimized, and the electron transition probability from the ground state to the excited state is decreased coincidentally from amyl to methyl. In other words, in view of exciting-light

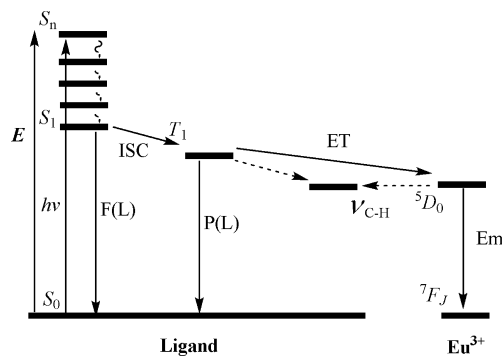


**Figure 4.** Schematic representation of the photophysical pathway of the Eu(III) complexes.

absorption, amyl substitution is the most favorable to the photoluminescence of the Eu(III) complexes.

Excited by near UV-light, all the  $Eu(N-Cx)_3phen$  complexes exhibit intense red emission. To investigate the photoluminescence mechanism of the Eu(III) organic complexes, the triplet state levels of the primary ligands N-Cx are the necessary evidence. The phosphorescence spectra of the  $Gd(N-Cx)_3 \cdot 2H_2O$  solid samples were measured at 10 K and were used to determine the triplet state levels. The radius of the  $Gd^{3+}$  ion (94 pm) was close to that of the  $Eu^{3+}$  ion (95 pm), so the coordination environments for the  $Gd^{3+}$  ion in  $Gd(N-Cx)_3 \cdot 2H_2O$  were similar to that for the  $Eu^{3+}$  ion in  $Eu(N-Cx)_3 \cdot 2H_2O$ . The lowest excited state energy level of the  $Gd^{3+}$  ion,  $6P_{7/2}$ , was about  $32\,000\text{ cm}^{-1}$ , much higher than that of the lowest triplet energy levels of N-Cx,  $T_1(L)$ , so the energy absorbed by N-Cx ligand cannot be transferred to the  $Gd^{3+}$  ion, and phosphorescence of N-Cx appears when  $Gd(N-Cx)_3 \cdot 2H_2O$  are excited by near-ultraviolet light of 397 nm. In this case, the lowest triplet state energies of the ligands N-Cx,  $T_1(L)$ , were determined by the shortest wavelength of the phosphorescence peaks to be 19 193, 18 181, 20 576, and 19 531  $\text{cm}^{-1}$ , all of which are higher than the lowest excited state of  $Eu^{3+}$ ,  $5D_0$  ( $17\,267\text{ cm}^{-1}$ ), and these triplet state levels demonstrate that the whole photoluminescence process of the Eu(III) complexes is adopted to a ligand-sensitized luminescence process (antenna effect).<sup>17</sup> The

overall photoluminescence process can be described as (1) after ligands N-Cx and phen absorb the exciting-light energy, electrons in ground state  $S_0$  of the ligand transit to the excited state  $S_n$ ; (2) excited electrons fall down to the  $S_1$  state through quick nonradiative transitions; (3) electrons transit to the lowest triplet state of the ligand [ $T_1(L)$ ] via an intersystem-cross (ISC); (4) energy is transferred to the lowest excited state ( $5D_0$ ) of the central  $Eu^{3+}$  ion in the complex molecule; (5) radiative transitions  $5D_0 \rightarrow 7F_J$  ( $J = 0-6$ ) happen, and the characteristic and narrow red fluorescence peaks of  $Eu^{3+}$  ion appear. However, there is a special effect for Eu(III) organic complexes that the C-H bond oscillation level in the organic ligands is just nearby the  $5D_0$  level of  $Eu^{3+}$ , so when the energy transfers from the  $T_1$  level of the ligands to the  $5D_0$  level of the Eu(III) central ion, the energy consumption would happen not only from the  $5D_0$  of  $Eu^{3+}$  to the C-H oscillators that are near to the  $Eu^{3+}$  ion<sup>18-20</sup> but also possibly from the  $T_1$  of the ligand to its own C-H bond oscillation in the carbazole ring. Therefore, C-H bond oscillator is another important factor affecting the photoluminescence intensity of the Eu(III) complexes. The whole photophysical pathway is shown in Figure 4.

The photoluminescence excitation (PLE) and emission (PL) spectra of the  $Eu(N-Cx)_3phen$  complexes are shown in Figure 5. The PLE spectra ( $\lambda_{em} = 613\text{ nm}$ ) show that the excitation band of  $Eu(N-C1)_3phen$  is the weakest, which is in accordance with the UV-vis absorption spectra in Figure 3. Under 397 nm NUV light excitation, the complexes show multiple narrow and intense emission peaks due to  $Eu^{3+} 5D_0 \rightarrow 7F_J$  transitions with all the strongest peaks locating at 613 nm ( $5D_0 \rightarrow 7F_2$  transition); this also reveals that different alkyl substituents at the N atom position did not change the site-symmetry around the  $Eu^{3+}$  ion, while the integrated emission intensity increases with the sequence:  $Eu(N-C2)_3phen > Eu(N-C3)_3phen > Eu(N-C5)_3phen > Eu(N-C1)_3phen$ . Meanwhile, all the complexes give the same CIE chromaticity coordinates ( $x = 0.67, y = 0.33$ ), which are actually the same as that of NTSC standard for red.

The overall luminescence quantum yield ( $\varphi_{lum}$ ) is in principle determined by the quantum yields of the intersystem crossing ( $\varphi_{ISC}$ ), the energy transfer steps ( $\varphi_{ET}$ ), and the luminescence efficiency of europium ion itself ( $\varphi_{Eu}$ ). Thus, the overall

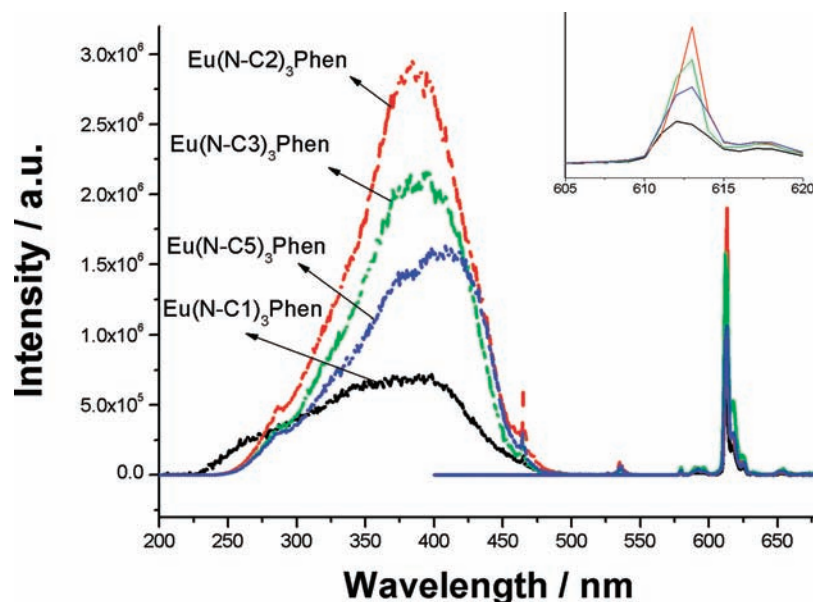


**Figure 5.** PLE ( $\lambda_{em} = 613\text{ nm}$ ) and PL ( $\lambda_{ex} = 397\text{ nm}$ ) spectra of the complexes  $Eu(N-C1)_3phen$ ,  $Eu(N-C2)_3phen$ ,  $Eu(N-C3)_3phen$ , and  $Eu(N-C5)_3phen$ .

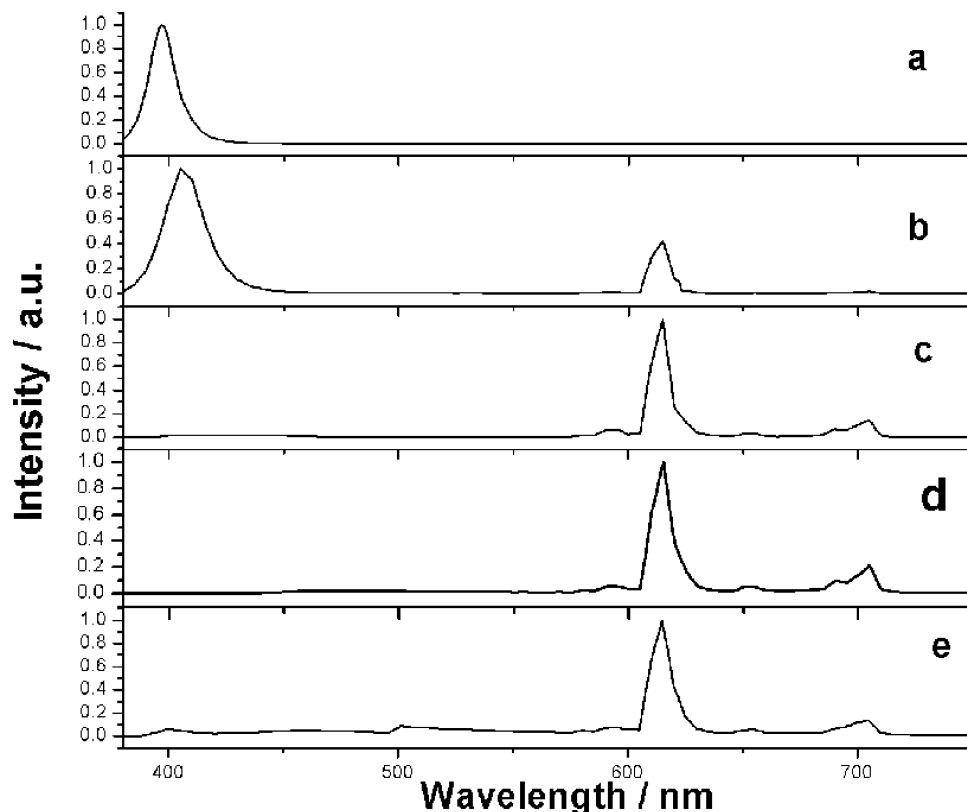


**Figure 6.** Emission spectra of the original NUV InGaN LED without phosphor (a), the LED with  $\text{Eu}(\text{N-C1})_3\text{phen}$  (b), the LED with  $\text{Eu}(\text{N-C2})_3\text{phen}$  (c), the LED with  $\text{Eu}(\text{N-C3})_3\text{phen}$  (d), and the LED with  $\text{Eu}(\text{N-C5})_3\text{phen}$  (e) under 20 mA forward bias.

luminescence quantum yield can be presented as the following equation:<sup>21</sup>

$$\varphi_{\text{lum}} = \varphi_{\text{ISC}}\varphi_{\text{ET}}\varphi_{\text{Eu}} \quad (1)$$

The emission intensity, determined by emitting photon number ( $I_{\text{em}}$ ) can be presented as the product of absorbed photon number ( $I_{\text{abs}}$ ) and the overall luminescence quantum yield ( $\varphi_{\text{lum}}$ ) as the following equation:<sup>22</sup>

$$I_{\text{em}} = I_{\text{abs}}\varphi_{\text{lum}} \quad (2)$$

Equation 2 indicates that the emission intensity is determined by two factors,  $I_{\text{abs}}$  and  $\varphi_{\text{lum}}$ . As shown in the UV-vis absorption spectra of the Eu(III) complexes (Figure 3 b), the absorbance of  $\text{Eu}(\text{N-Cx})_3\text{phen}$  decreases in the order  $\text{Eu}(\text{N-C5})_3\text{phen} > \text{Eu}(\text{N-C3})_3\text{phen} > \text{Eu}(\text{N-C2})_3\text{phen} > \text{Eu}(\text{N-C1})_3\text{phen}$ . This sequence means a bigger alkyl substituent group at the N position would increase the molar absorption coefficient  $\epsilon$  and thus increase  $I_{\text{abs}}$  of the corresponding Eu(III) complex. However, another effect happens synchronously since the amount of C-H bonds increases at the same time, and therefore the  $\varphi_{\text{ET}}$  would decrease due to the enhanced C-H bond oscillation, resulting in decrease of the  $\varphi_{\text{lum}}$ . The quantum yields of the complexes  $\text{Eu}(\text{N-C1})_3\text{phen}$ ,  $\text{Eu}(\text{N-C2})_3\text{phen}$ ,  $\text{Eu}(\text{N-C3})_3\text{phen}$ , and  $\text{Eu}(\text{N-C5})_3\text{phen}$ , measured in the solid state using an integrating sphere with a similar method described by Lin,<sup>23</sup> respectively are 0.25, 0.19, 0.14, and 0.12, which is consistent with the deduction above-mentioned from the C-H bond oscillation. Hence we can conclude, along with the enlargement of the alkyl at the N-position in the carbazole ring, the whole photoluminescence process exhibits as a competition between

the absorption capacity determined by  $I_{\text{abs}}$ , and the energy transfer efficiency that would be reduced by C-H bond oscillation, expressed by  $\varphi_{\text{lum}}$ . As a competition consequence,  $\text{Eu}(\text{N-C2})_3\text{phen}$  with ethyl at the N-position shows the highest emission intensity, and the total sequence of the emission intensity is  $\text{Eu}(\text{N-C2})_3\text{phen} > \text{Eu}(\text{N-C3})_3\text{phen} > \text{Eu}(\text{N-C5})_3\text{phen} > \text{Eu}(\text{N-C1})_3\text{phen}$ , as shown in Figure 5 (right and insert).

The decay times for  ${}^5\text{D}_0 \rightarrow {}^7\text{F}_2$  transition (613 nm) of the  $\text{Eu}^{3+}$  in  $\text{Eu}(\text{N-Cx})_3\text{phen}$  were measured, and the lifetime values were 512, 766, 1010, and 750  $\mu\text{s}$  for  $x = 1, 2, 3,$  and  $5,$  respectively. All the curves were fitted with a single-exponential function, indicating that the  $\text{Eu}^{3+}$  ions in their complexes molecule occupied sites with the same symmetry.

$\text{Eu}(\text{N-Cx})_3\text{phen}$  were used as phosphor in the same mass ratio of 1:20 of phosphor to silica gel to fabricate LED with an  $\sim 395$  nm emitting InGaN chip. The emission spectra of original LED without phosphor and the LEDs with the complexes under 20 mA forward bias are shown in Figure 6. The LED with  $\text{Eu}(\text{N-C1})_3\text{phen}$  (Figure 6b) only absorbs a little 395 nm light from the chip because of its low absorption capacity. All the LEDs with  $\text{Eu}(\text{N-Cx})_3\text{phen}$  exhibit sharp and intense red-emission peaks centering at 613 nm due to the  $\text{Eu}^{3+}$  emission from the complexes.

## Conclusions

A series of carbazole-based  $\beta$ -diketonate derivatives and their europium(III) ternary complexes  $\text{Eu}(\text{N-Cx})_3\text{phen}$  were synthesized. All complexes show high thermal stability and intense red emission under NUV excitation. There exists a competition between the absorption capacity and the energy transfer efficiency as the alkyl substituent at the N-position in the carbazole ring of the complexes changes, and as a consequence, the total sequence of the emission intensity is  $\text{Eu}(\text{N-C2})_3\text{phen} > \text{Eu}(\text{N-C3})_3\text{phen} > \text{Eu}(\text{N-C5})_3\text{phen} > \text{Eu}(\text{N-C1})_3\text{phen}$ .

C3)phen > Eu(N-C5)<sub>3</sub>phen > Eu(N-C1)<sub>3</sub>phen. Bright red LEDs with the complexes as phosphors were fabricated. All the results indicate that the europium(III) complexes are promising candidates as red components for fabrication of NUV-based white LEDs.

**Acknowledgment.** This work was funded by research grants from the Natural Science Foundation of China (No. 50672136) and the Chinese Postdoctoral Research Funds (No. 20080440785).

## References and Notes

- (1) Yang, J. X.; Tao, X. T.; Yuan, C. X.; Yan, Y. X.; Wang, L.; Liu, Z.; Ren, Y.; Jiang, M. H. *J. Am. Chem. Soc.* **2005**, *127*, 3278.
- (2) Hasnaoui, K.; Zgou, H.; Hamidi, M.; Bouachrine, M. *Chin. Chem. Lett.* **2008**, *19*, 488.
- (3) Wong, W.; Ho, C.; Gao, Z.; Mi, B.; Chen, C.; Cheah, K.; Lin, Z. *Angew. Chem., Int. Ed.* **2006**, *45*, 7800.
- (4) Ho, C.; Wong, W.; Wang, Q.; Ma, D.; Wang, L.; Lin, Z. *Adv. Funct. Mater.* **2008**, *18*, 928.
- (5) Ho, C.; Lin, M.; Wong, W.; Wong, W.; Chen, C. H. *Appl. Phys. Lett.* **2008**, *92*, 083301.
- (6) Aly, S. M.; Ho, C.; Fortin, D.; Wong, W.; Abd-El-Aziz, A. S.; Harvey, P. D. *Chem.—Eur. J.* **2008**, *14*, 8341.
- (7) Wong, W. *Coord. Chem. Rev.* **2005**, *249*, 971.
- (8) Wong, W.; Ho, C. *Coord. Chem. Rev.* **2006**, *250*, 2627.
- (9) Morin, J.; Leclerc, M.; Ade's, D.; Siove, A. *Macromol. Rapid Commun.* **2005**, *26*, 761.
- (10) Xiang, N. J.; Leung, L. M.; So, S. K.; Wang, J.; Su, Q.; Gong, M. L. *Mater. Lett.* **2006**, *60*, 2909.
- (11) Lee, K. M.; Cheah, K. W.; An, B. L.; Gong, M. L.; Liu, Y. L. *Appl. Phys. A: Mater. Sci. Process.* **2005**, *A80*, 337.
- (12) Iwanaga, H.; Amano, A.; Aiga, F.; Harada, K.; Oguchi, M. *J. Alloys Compd.* **2006**, *408*, 921.
- (13) He, P.; Wang, H.; Liu, S.; Hu, W.; Shi, J.; Wang, G.; Gong, M. J. *Electrochem. Soc.* **2009**, *156*, E46.
- (14) He, P.; Wang, H.; Liu, S.; Shi, J.; Wang, G.; Gong, M. *Electrochem. Solid St.* **2009**, *12*, B61.
- (15) Xiang, N.; Xu, Y.; Wang, Z.; Wang, X.; Leung, L. M.; Wang, J.; Su, Q.; Gong, M. *Spectrochim. Acta, Part A* **2008**, *69*, 1150.
- (16) Grigalevicius, S. *Synth. Met.* **2006**, *156*, 1.
- (17) Aiga, F.; Iwanaga, H.; Amano, A. *J. Phys. Chem. A* **2005**, *109*, 11312.
- (18) Horrocks, W. D., Jr.; Sudnick, D. R. *J. Am. Chem. Soc.* **1979**, *101*, 334.
- (19) Horrocks, W. D., Jr.; Sudnick, D. R. *Acc. Chem. Res.* **1981**, *14*, 384.
- (20) Beeby, A.; Clarkson, I. M.; Dickins, R. S.; Faulkner, S.; Parker, D.; Royle, L.; Sousa, A. S.; Williams, J. A. G.; Woods, M. *J. Chem. Soc., Perkin Trans.* **1999**, *2*, 493.
- (21) Xiang, N.; Leung, L. M.; So, S.; Gong, M. *Spectrochim. Acta, Part A* **2006**, *65*, 907.
- (22) Ferreira, L. F. V.; Branco, T. J. F.; Rego, A. M. B. *ChemPhysChem* **2004**, *5*, 1848–1854.
- (23) Lin, H.; Wang, H. Y.; Li, C. M.; Li, X. J.; Tanabe, S.; Yu, J. Y. *Spectrochim. Acta, Part A* **2007**, *67*, 1417.

JP908416Q